Multi-tier Priority Queues & 2-tier Ladder Queue for Managing Pending Events in Sequential & Optimistic Parallel Simulations

Julius D. Higiro

A thesis proposal submitted for the degree of Master of Science in Computer Science

May 2017

1 Introduction

Discrete event simulation (DES) is the simulation of a discrete event system that contains states that operate at discrete time steps [1]. At each point in time in a simulation, a virtual time-stamp is assigned to an event and the event precipitates a transition from one state to another state. This change in system state is used to represent the dynamic nature and behavior of a real-world system [2]. DES has been used in a variety of fields in academia, industry and the public sector as a tool to help inform our knowledge of discrete event systems and to improve decision-making processes [1]. DES provides an effective means for analyzing real or artificial systems without the constraint of limited resources such as time, financial costs, or safety. For example, the simulation of a battlefield environment can deliver insightful information to military planners on enemy troop movements, tactics and capabilities during strategic planning efforts [3]. A discrete event simulation of the battlefield allows military leaders to examine the impacts of decisions without the real-world risks associated with committing forces to dangerous environments.

Parallelism in computing frameworks that support DES increase performance throughput that is needed to construct and execute large scale and complex simulation models. With the growth and prevalence of semiconductor technology, cheaper and powerful multi-processors can be instrumented to achieve greater computing power for parallel discrete event simulations (PDES). However, the speedup achieved using multi-core and multi-processor systems requires efficient parallel programs.

Sequential and parallel DES are designed as a set of logical processes (LPs) that interact with each other by exchanging and processing timestamped events or messages [4]. Events that are yet to be processed are called "pending events". Pending events must be processed by LPs in priority order to maintain causality, with event priorities being determined by their timestamps. Consequently, data structures for managing and prioritizing pending events play a critical role in ensuring efficient sequential and parallel simulations [5, 6, 7, 8]. The effectiveness of data structures for event management is a conspicuous issue in larger simulations, where thousands or millions of events can be pending [9, 10]. Large pending event sets can arise when a model has many LPs or when each LP generates / processes many events. Overheads in managing pending events is magnified in fine grained simulations where the time taken to process an event is very short. Furthermore, the synchronization strategy used in PDES, Time Warp as described in section 2, can further impact the effectiveness of the data structure due to additional processing required for rollback-based recovery.

1.1 Motivations

Many investigations have explored the effectiveness of a wide variety of data structures for managing the pending event set as discussed in Section 5. Among the various data structures, the Ladder Queue proposed by Tang et al., [11] has shown to be the most effective data structure for managing pending events [12, 8], particularly in sequential DES. Accordingly, we aim to replace the heap-based data structures used in our Time Warp synchronized parallel simulator with the Ladder Queue. Section 4.5 discusses our Ladder Queue implementation and its fine-tuning. The Ladder Queue outperformed our multi-tier heap-based data structures in certain sequential simulations, consistent with observations by other investigators [8, 10]. However, as detailed in section 6, the Ladder Queue was substantially slower in two cases – ❶ high concurrency: larger number of concurrent events (i.e. events with same time-stamp) per LP, and ❷ Time Warp synchronized parallel simulations conducted on a distributed memory computing cluster. Conversely, our multi-tier data structures performed well in parallel simulations.

To provide a good balance for both sequential and optimistic parallel simulations, we propose a significant change to the design of the Ladder Queue. Our revised data structure, discussed in Section 4.6, is called 2-tier Ladder Queue (2tLadderQ). Various configurations of the standard PHOLD benchmark are used to assess the effectiveness of the multi-tier data structures vs. our fine-tuned implementation of the Ladder Queue. The preliminary results from our experiments discussed in Section 6 shows 2tLadderQ provides comparable performance in sequential simulations but outperforms the Ladder Queue in optimistic parallel simulations. Our 3-tier heap (3tHeap) outperforms our 2tLadderQ in high concurrency scenarios.

2 Miami University Simulation Environment (MUSE)

The implementation and assessment of the different data structures was conducted using our parallel simulation framework called MUSE. It has been developed in C++ and uses the Message Passing Interface (MPI) library for parallel processing. MUSE uses Time Warp and standard state saving approach to accomplish optimistic synchronization of the LPs to maintain causality in event processing.

In a Time Warp based simulation such as MUSE, the simulation is organized as a set of LPs that interact with each other by exchanging virtual times-tamped events. LPs process events in non-decreasing receive-time order and generate new events that are transmitted to LPs on local or remote processors. Synchronization of event processing is achieved through the adherence to the local causality constraint, which requires that LPs only process events in Least Time-stamp First (LTSF) order [4].

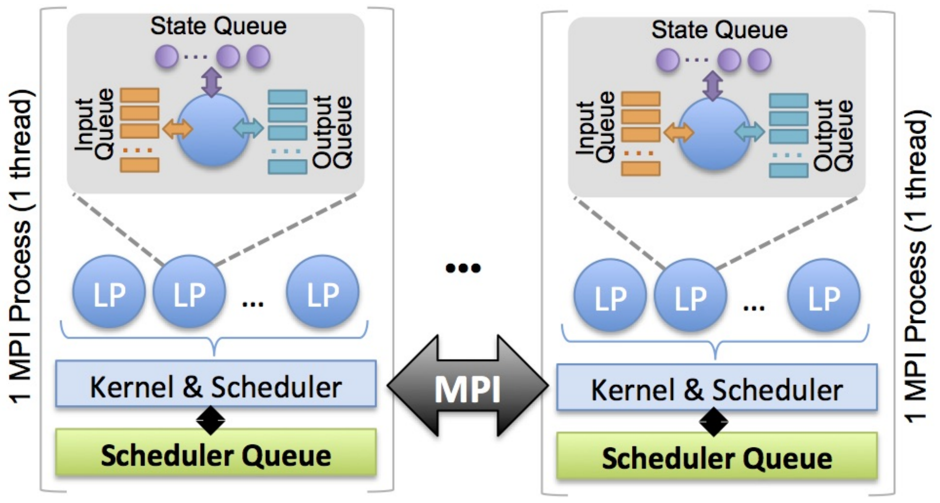

Figure 1: Overview of a parallel MUSE simulation

In contrast to the conservative synchronization protocol that blocks event processing until it is guaranteed that an LP cannot receive a future event with a receive-time lesser than it's LVT (altogether avoiding the manifestation of causality errors) [4]. Time Warp simulations are able to withstand violations of the causality constraint. Time Warp LPs proceed optimistically with event processing and in the event that it encounters an event (*named a* ***straggler***) with a receive time lesser than the LVT, a rollback operation is performed. A rollback requires that an LP undo all event processing that occurred at the LVT equal to the straggler time stamp and forward. The LP performs a rollback to a state with an LVT preceding the straggler time stamp and it sends an anti-message to all other agents with the purpose of cancelling the previously sent events.

A conceptual overview of a parallel simulation is shown in Figure 2. The simulation kernel implements core functionality associated with LP registration, event processing, state saving, synchronization and Global Virtual Time (GVT) garbage based collection. Each LP in a simulation maintains an input, output and state queue. The input queue is used to handle pending events that have yet to be processed. The output queue stores anti-messages, which are events that are sent to other LPs to cancel out previously sent events. The state queue stores the state of the LP at each discrete point in virtual simulation time. A Time Warp LP also maintains a local virtual time (LVT) that is updated to the time-stamp of the event most recently processed by the LP.

The kernel uses a centralized LTSF scheduler queue for managing pending events and scheduling event processing for local LPs. LPs are permitted to generate events only into the future –*i.e.,* the time stamp on events must be greater than their Local Virtual Time (LVT). Consequently, with a centralized LTSF scheduler, event exchanges between local LPs cannot cause rollbacks. Only events received via MPI can cause rollbacks in our simulation. The scheduler is designed to permit different data structures to be used for managing pending events. This feature is used to experiment with the different pending event scheduler queues discussed in Section 4. A scheduler queue is required to implement the following key operations to manage pending events:

❶ **Enqueue one or more future events**: This operation adds the given set of events to the pending event set. Multiple events are added to reprocess events after a rollback.

❷ **Peek next event**: This operation is expected to return the next event to be processed. This information is used to determine next LP and to update its LVT prior to event processing. Note that peek does not dequeue events.

❸ **Dequeue events for next LP**: In contrast to peek, this operation is expected to dequeue the events to be dispatched for processing by an LP. This operation is performed by the kernel immediately after a peek operation. The operation must dequeue the next set of concurrent events, *i.e.,* events with the same receive time sent to an LP. However, the concurrent events could have been sent by different LPs on different MPI-processes. Dispatching concurrent events in a single batch streamlines modeling broad range of scenarios. An total order within concurrent events is not imposed but can be readily introduced if needed.

❹ **Cancel pending events**: This operation is used as part of rollback recovery process to aggressively remove *all pending events* sent by a given LP ($\mathrm{LP}_{\mathrm{sender}}$) to another LP ($\mathrm{LP}_{\mathrm{dest}}$) at-or-after a given time ($t_{rollback}$). In our implementation, only one anti-message with send time $t_{rollback}$ is dispatched to $\mathrm{LP}_{\mathrm{dest}}$ from $\mathrm{LP}_{\mathrm{sender}}$ to cancel prior events sent by $\mathrm{LP}_{\mathrm{sender}}$ to $\mathrm{LP}_{\mathrm{dest}}$ at-or-after $t_{rollback}$. This is a contrast to conventional aggressive cancellation in which one anti-message is generated per event. This feature short circuits the need to send a large number of anti-messages thereby enabling faster rollback recovery. This feature also reduces scans required to cancel events in Ladder Queue data structures discussed in Section 4.5 and Section 4.6. Note that this feature is reliant on the First-In-First-Out (FIFO) communication guarantee provided by MPI.

2.1 Experimental Platform

The design of MUSE and the experiments reported were conducted using a distributed-memory compute cluster consisting of 80 compute nodes interconnected by 1 GBPS Ethernet. Each compute node has 8 cores from two quad-core Intel Xeon ®CPUs (E5520) running at 2.27 GHz with hyper-threading disabled. Each compute node has 32 GB of RAM (4 GB per core) in Non-Uniform Memory Access (NUMA) configuration. The cluster has an independent 1 GBPS Ethernet network to support a shared file system. The nodes run Red Hat Enterprise Linux 6, with Linux (kernel ver 2.6.32) and the cluster runs PBS/Torque. The simulation software was compiled using GCC version 4.9.2 (**-O3** optimization) with OpenMPI 1.6.4. All debug assertions were turned off for maximum performance.

3 Simulation Models

3.1 Parallel HOLD (PHOLD)

The experimental analysis have been conducted using a parallelized version of the classic Hold synthetic benchmark called PHOLD. It has been used by many investigators because it has shown to effectively emulate the steady-state phase of a typical simulation [8, 11]. Our PHOLD implementation developed using MUSE provides several parameters (specified as command-line arguments) summarized in table 1. The benchmark consists of a 2-dimensional grid of LPs specified via the **rows** and **cols** parameters. The LPs are evenly partitioned across the MPI-processes used for simulation. The **imbalance** parameter influences the partition, with larger values skewing the partition as shown in Figure3.1(a). The **imbalance** parameter has no impact in sequential simulations.

Table 1: Parameters in PHOLD benchmark

Parameter	Description
rows	Total number of rows in model.
cols	Total number of columns in model. #LPs = **rows** $\times$ **cols**
eventsPerLP	Initial number of events per LP.
delay or λ	Value used with distribution – Lambda (λ) value for exponential distribution *i.e.,* $P(x\|\lambda) = \lambda e^{-\lambda x}$.
%selfEvents	Fraction of events LPs send to self
granularity	Additional compute load per event.
imbalance	Fractional imbalance in partition to have more LPs on a MPI-process.
simEndTime	GVT when simulation logically ends.

The PHOLD simulation commences with a fixed number of events for each LP, specified by the **eventsPerLP** parameter. For each event received by an LP a fixed number of trigonometric operations determined by **gran-**

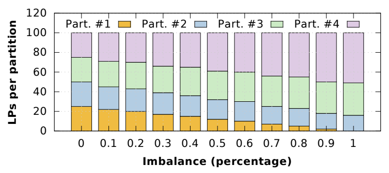

(a) Impact of **imbalance**

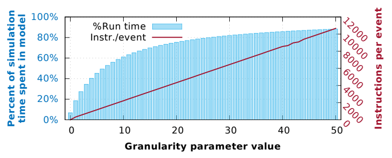

(b) Impact of **granularity**

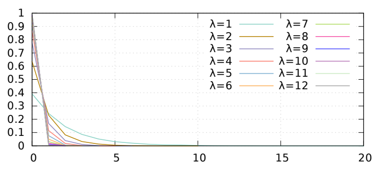

(c) Impact of **delay** (λ)

Figure 2: Impact of varying key parameter values in the PHOLD model

ularity are performed to place CPU load. The impact of increasing the **granularity** parameter (no unit) is summarized in Figure 2(b) – smaller values result in finer grained simulations. For each event, an LP schedules another event to a randomly chosen adjacent LP. The **selfEvents** parameter controls the fraction of events that an LP schedules to itself. The event timestamps are determined by a given **delay-distrib** and **delay** or λ parameters. Our experiments use an exponential distribution for timestamps, because it has shown to reflect event distribution commonly found in a broad range of simulation models [11]. Time stamp of events is computed as t_{recv} = LVT + 1 + $\lambda e^{-\lambda x}$. The impact of changing the λ (*i.e.*, **delay**) is shown in Figure 3.1(c) –smaller values of λ provide a broader range of time stamp value for future events resulting in fewer concurrent events per LVT. Conversely, larger λ values cause timestamps to be close to the current epoch, increasing both the number of concurrent events per LVT and the possibility of rollbacks. Section 6 explores impact of these parameters on scheduler queue performance using 2,500 different configurations.

4 Scheduler Queues

The pending events are managed by different scheduler queues that utilize different data structures to implement the key operations discussed in Section 4, namely: enqueue, peek dequeue, and cancel. In this study we have compared the effectiveness of 6 different non-intrusive queue data structures namely: ① binary heap (**heap**), ② 2-tier heap (**2tHeap**), ③ 2-tier Fibonacci heap (**fibHeap**), ④ 3-tier heap (**3tHeap**), ⑤ Ladder Queue (**ladderQ**), and ⑥ 2-tier Ladder Queue (**2tLadderQ**). The queues are broadly classified into two categories, namely: single-tier and multi-tier queues. Single-tier queues such as **heap** use only a single data structure for accomplishing the 4 key operations. Conversely, multi-tier queues organize events into tiers, with each tier implemented using different data structures. Table 4 summarizes the algorithmic time complexities of the 6 data structures discussed in the following subsections.

Table 2: Comparison of algorithmic time complexities of different data structures

Legend – l: #LPs, e: #events / LP, c: #concurrent events, z: #canceled events, ${}_{\mathrm{t2}}k$: parameter, 1^*: amortized constant

Name	Enqueue	Dequeue	Cancel
heap	$\log(e \cdot l)$	$\log(e \cdot l)$	$z \cdot \log(e \cdot l)$
2tHeap	$\log(e)+ \log(l)$	$\log(e)+ \log(l)$	$z \cdot \log(e)+ \log(l)$
fibHeap	$\log(e) + 1^*$	$\log(e) + 1^*$	$z \cdot \log(e) + 1^*$
3tHeap	$\log(\frac{e}{c}) + \log(l)$	$\log(l)$	$e + \log(l)$
ladderQ	1^*	1^*	$e \cdot l$
2tLadderQ	1^*	1^*	$e \cdot l \div {}_{\mathrm{t2}}k$

4.1 Binary Heap (heap)

The binary heap based (**heap**) is a commonly used data structure for implementing priority queues. It is a single tier-data structure and is implemented using a conventional array-based approach. A **std::vector** is used as the backing container and algorithms (**std::push_heap**, **std::pop_heap**) are used to maintain the heap. The heap is prioritized on both time stamp and LP's *ID* (to dequeue batches of events), with lowest time stamp at the root of the heap. Operations on the heap are logarithmic in time complexity – given l LPs each with e events/LP, the time complexity of enqueue and dequeue operations is $\log(e \cdot l)$ as shown in Table 4. If event cancellation requires z events to be removed from the heap, the time complexity is $z \cdot \log(e \cdot l)$. Consequently, for long or cascading rollbacks the cancellation costs is high.

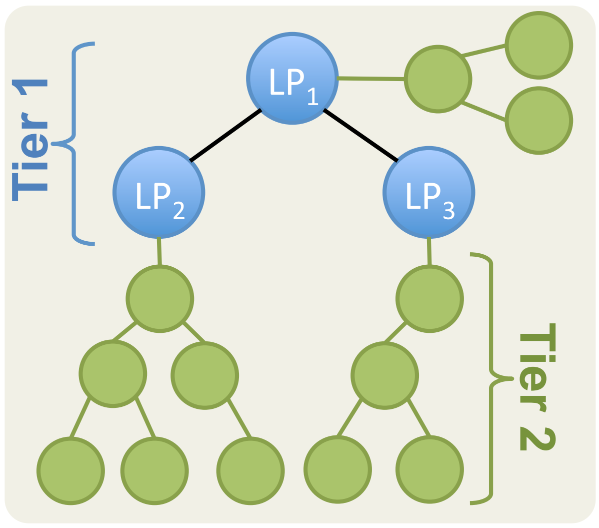

(a) 2-tier Heap

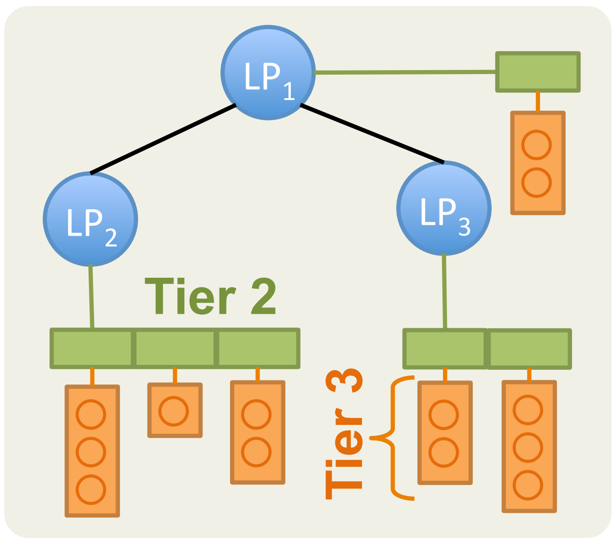

(b) 3-tier Heap

Figure 3: Structure of 2-tier & 3-tier heap

4.2 Two-tier Heap (2tHeap)

The **2tHeap** is designed to reduce the time complexity of cancel operations by subdividing events into two distinct tiers as shown in Figure 4.1. The first tier has containers for each local LP on an MPI-process. Each of the tier-1 containers contain a heap of events to be processed by a given LP. In **2tHeap** both tiers are maintained as independent binary heaps. Consequently, given l LPs and e pending events per LP, enqueue and dequeue operates require $\log e$ time to insert in tier-2 followed by $\log l$ time to reschedule the LP. Note that the tier-1 heap is updated only if the root event in tier-2 changes after an operation. Consequently, the best case time complexity becomes $\log e$ when compared to $\log e \cdot l$ for the **heap**. Furthermore, cancellation of events for an anti-message is restricted to just the tier-2 entries of LP $_{\text{dest}}$ (see section 2) with utmost 1 tier-1 operation to update schedule position of LP $_{\text{dest}}$. A **std::vector** is used as the backing storage for both tiers and standard algorithms are used to maintain the min-heap property for both tiers after each operation.

4.3 2-tier Fibonacci Heap (fibHeap)

The **fibHeap** is an extension to the previous **2tHeap** data structure and uses a Fibonacci heap for scheduling LPs. The Fibonacci heap is a slightly modified version from the BOOST C++ library. The Fibonacci heap has an amortized constant time for changing key values and finding minimum. Consequently, we use it for the first tier which is responsible for scheduling LPs and use a standard binary heap for the second tier. We do not use Fibonacci heap for the second tier because we found its runtime constants to be higher than a binary heap. Accordingly, the time complexity for enqueue and dequeue operations is $\log(e) + 1^*$.

4.4 Three-tier Heap (3tHeap)

The **3tHeap** builds upon **2tHeap** by further subdividing the second tier into two tiers as shown in Figure 4.1(b). The binary heap implementation for the first tier that manages LPs for scheduling has been retained from **2tHeap**. However, the 2nd tier is implemented as a list of containers sorted based on receive time of events. Each tier-2 container has a 3rd tier list of concurrent events. Assuming each LP has c concurrent events on an average, there are $\frac{e}{c}$ tier-2 entries with each one having c pending events. Inserting events in the **3tHeap** is accomplished via binary search at tier-2 with time complexity $\log \frac{e}{c}$ followed by an append to tier-3, a constant time operation. Enqueue to tier-2 is followed by an optional heap fix-up of time complexity $\log l$ as summarized in Table 4. Dequeue operation for a LP removes a tier-2 entry in constant time followed by a $\log l$ heap fix-up for scheduling. Event cancellation has time complexity of $e + \log(l)$ as it requires inspecting each event in tier-3 followed by heap fix-up. As an implementation optimization, we recycle tier-2 containers to reduce allocation and deallocation overhead.

4.5 Ladder Queue (ladderQ)

The **ladderQ** is a priority queue implementation proposed by Tang et al [11] with amortized constant time complexity as summarized in Table 4. Several investigators have independently verified that for sequential DES the **ladderQ** outperforms other priority queues, including: simple sorted list, binary heap, Splay tree, Calendar queue, and other multi-list data structures [12, 8, 11]. There are two key ideas underlying the Ladder Queue, namely: ① minimize the number of events to be sorted and ② delay sorting of events as much as possible. The multi-tier data structures also aim to minimize the number of events to be sorted. However, in contrast to the **ladderQ**, the other data structures always fix-up and maintain a minimum heap property. The ladder queue consists of the following 3 substructures:

1. *Top*: An unsorted list which contains events scheduled into the distant future or epoch.
2. *Ladder*: Consists of multiple rungs, *i.e.,*list of buckets. Each bucket contains list of events with a finite range of time stamp values. Hence, although events within a bucket are not sorted, the buckets on a rung are organized in a sorted order. The **ladderQ** minimizes the number of events to be finally sorted by

recursively breaking large buckets into smaller buckets in lower rungs of its ladder. Lower rungs in the ladder have smaller buckets with smaller time ranges.

3. *Bottom*: This substructure contains a sorted list of events to be processed. Inserts into *Bottom* must preserve sorted order. Hence, the **ladderQ** strives to maintain a short bottom by moving events back into the ladder, as needed [11].

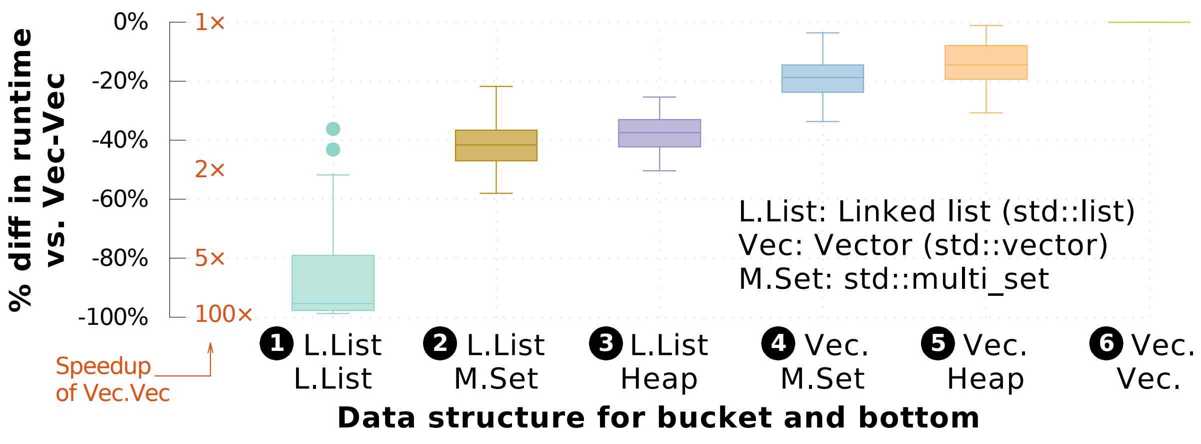

(a) Comparison sequential runtimes

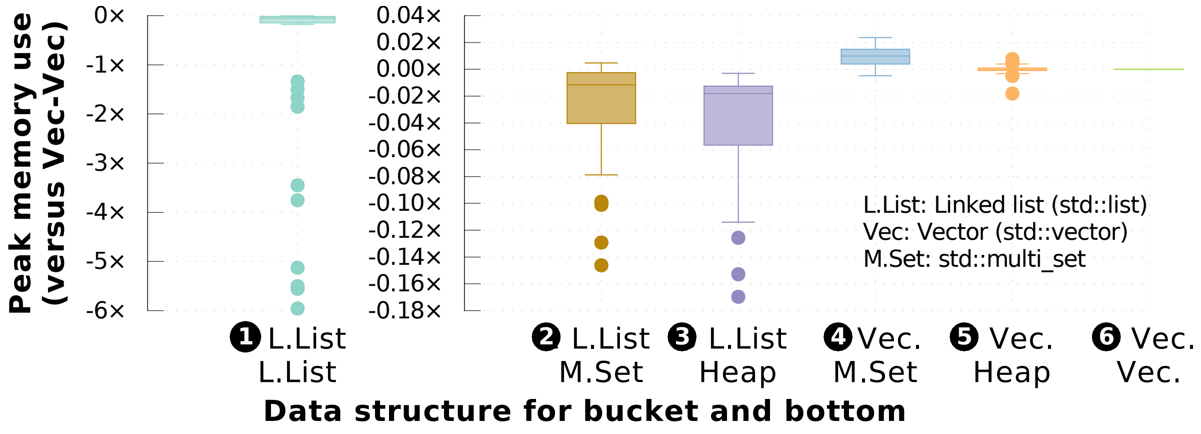

(b) Peak memory used

Figure 4: Comparison of execution time and peak memory for PHOLD benchmark (different parameter settings) using 6 different ladderQ configurations

4.5.1 Fine tuning Ladder Queue performance

Our implementation closely followed the design in the original paper by Tang et al [11]. However, to minimize runtime constants, we have explored different configurations for the buckets and the *Bottom* in the **ladderQ**. Specifically, we have explored the following 6 configurations – ❶ L.List-L.List: using a doubly-linked list (L.List) implemented by **std::list**) for buckets and bottom. Events are inserted into bottom via linear search as proposed by Tang et al. ❷ L.List-M.Set: L.List for buckets and a Multi-set ($\log n$ operations) for bottom, ❸ L.List-Heap: a L.List and a binary heap (backed by a **std::vector**) for bottom, ❹ Vec-M.Set: a dynamically growing array (*i.e.,* **std::vector**) for buckets and Multi-set bottom, ❺ Vec-Heap: Vector buckets and binary heap for bottom, and ❻ Vec-Vec: Vector for buckets and bottom. This configuration enables using quick sort(*i.e.,* **std::sort**) for sorting buckets and binary search for inserting events into bottom.

Runtime comparison of the 6 **ladderQ** configurations is summarized in Figure 4.5. The data was obtained using **PHOLD** with different parameter settings. The ❻th Vec-Vec configuration was the fastest and performance of other configurations are shown relative to it in Figure 4.5(a). The L.List-L.List configuration was generally the slowest and performed 85 ×(or 98%) slower than the Vec-Vec configuration. The peak memory used for simulations is shown in Figure 4.5(b), in comparison with the Vec-Vec configuration. As shown by the charts in Figure 4.5, the increased performance of Vec-Vec comes at about a 6×increase in peak memory footprint when compared to L.List-L.List configuration. This increased footprint arises because the **std::vector** internally doubles its capacity as it grows. With many buckets in the **ladderQ**, each implemented using a **std::vector**, the overall peak memory footprint is higher. Certainly, the increased capacity is used if the number of events in buckets grow. However, the Vec-M.Set and Vec-Heap configurations consume a bit more memory in some configurations, showing that Vec-Vec is not the worst in memory consumption. Consequently, we use the Vec-Vec configuration as it provides the fastest performance among the 6 configurations.

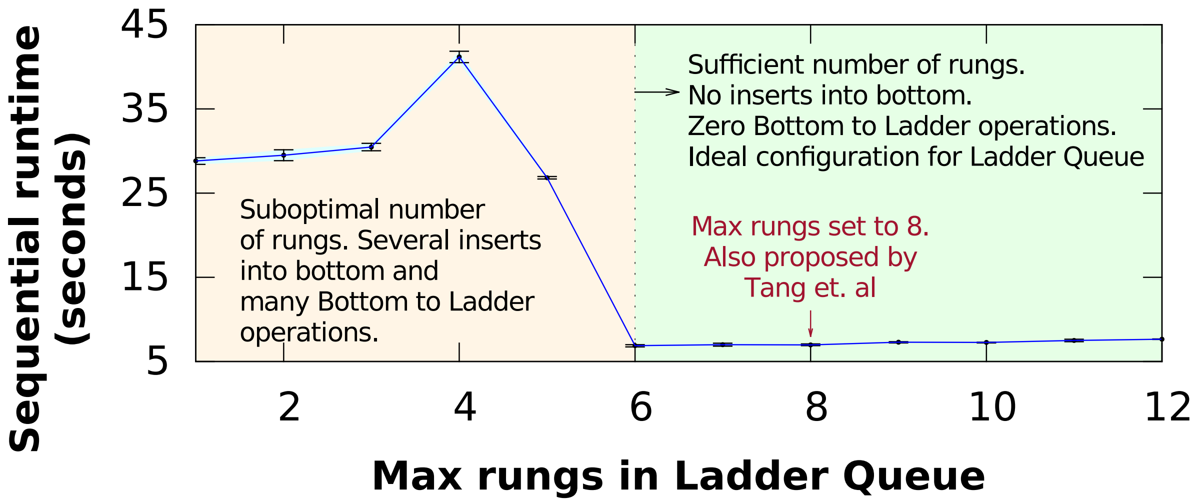

Figure 5: Impact of limiting rungs in Ladder

The maximum number of rungs in the *Ladder* also influences the overall performance of the **ladderQ** [11]. The chart in Figure 4.5.1 illustrates the impact of limiting the maximum number of rungs in the **ladderQ**. When the rungs are too few, the timestamp-based width of buckets is larger and more events with many different timestamps are packed into buckets. This also causes the *Bottom* to be longer with events spanning a broader range of timestamps. Consequently, when inserts happen into *Bottom*, many *Bottom*-to-*Ladder* re-bucketing operations are triggered to ensure bottom is short. These re-bucketing operations with many events significantly degrade performance. However, once sufficient number of rungs (6 rungs in this case) are permitted the events are better subdivide into smaller timestamp-based bucket widths. Small bucket widths in turn minimize inserts into bottom and *Bottom*-to-*Ladder* operations, ensuring good performance.

The chart in Figure 4.5.1 shows that a minimum of 6 rungs is required. For some select configurations of larger models we observed (data not shown) that 5 rungs would be sufficient. However, the number of rungs cannot exceed beyond a threshold to avoid infinite spawning of rungs [11]. Moreover, it limits the overheads involved in re-bucketing events from rung-to-rung [11]. Accordingly, based on the observations in figure 4.5.1, we decided to adopt a maximum of 8 rungs, consistent with the threshold proposed by Tang et al [11]. Furthermore, we trigger *Bottom*-to-*Ladder* re-bucketing only if the *Bottom* has events at different timestamps to further reduce inefficiencies.

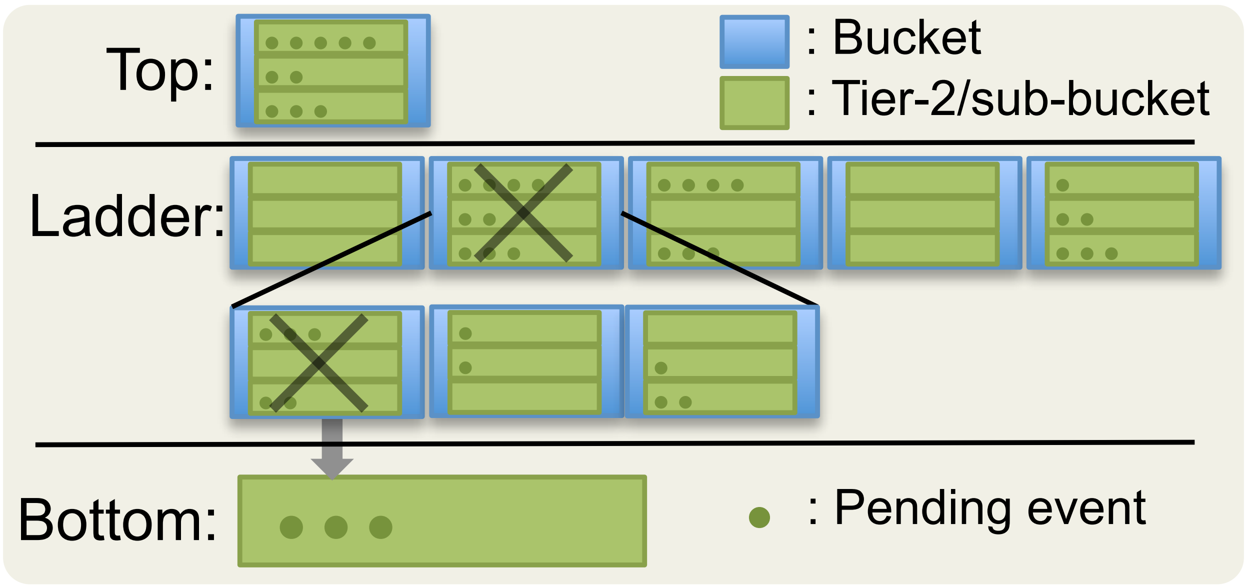

Figure 6: Structure of 2-tier Ladder Queue (2tLadderQ) with 3 sub-buckets / bucket (*i.e.,* $_{t2}$ k=3)

4.5.2 Shortcoming of Ladder Queue for optimistic PDES

The amortized constant time complexity of enqueue and dequeue operations enable the **ladderQ** to outperform other data structures in sequential simulations [12, 8, 11]. However, canceling events, requires a linear scan of pending events because *Top* and buckets in rungs are not sorted. In practice, scans of *Top*, *Ladder* rung buckets, and *Bottom* can be avoided based on cancellation times. Nevertheless, in a general case, event cancellation time complexity is proportional to the number of pending events – *i.e.,* $e \cdot l$ as summarized in Table 4. This issue is exacerbated in large simulations where thousands of events are typically present in *Top* and buckets in various rungs.

In this context, it is important to recollect from Section 2 that – as an optimization, **MUSE** utilizes only one anti-message to from LP $_{\text{sender}}$ to LP $_{\text{dest}}$ to cancel all n events sent after $t_{rollback}$ (rather than sending n individual anti-messages) which reduces overheads. Furthermore, with our centralized scheduler design, only events received from LPs on other MPI-processes can trigger rollbacks. Consequently, the number of scans of the **ladderQ** that actually occur is significantly fewer in our case, despite the aggressive cancellation strategy.

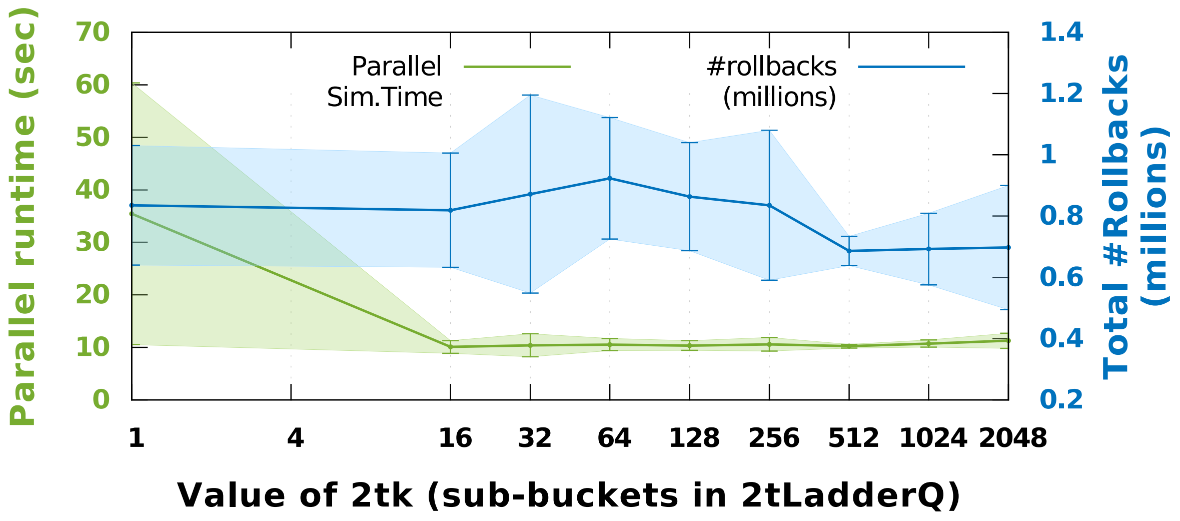

Figure 7: Effect of varying tk

4.6 2-tier Ladder Queue (2tLadderQ)

A key shortcoming of the Ladder Queue for Time Warp based optimistic PDES arises from the overhead of canceling events used for rollback recovery. Our experiments (see Section 6) show that event cancellation overhead of **ladderQ** is a significant bottleneck in parallel simulation. On the other hand, our multi-tier data structures, where pending events are more organized, performed well.

Consequently, to reduce cost of event cancellation, we propose a 2-tier Ladder Queue (**2tLadderQ**) in which each bucket in *Top* and *Ladder* is further subdivided into $_{tk}$ sub-buckets, where $_{tk}$ is specified by the user. Figure 4.5.2 illustrates an overview of the **2tLadderQ** with $_{tk} = 3$ sub-buckets in each bucket. Given a bucket, a hash of the sending LP's ID (or the receiver LP ID, one or the other but not both) is used to locate a sub-bucket into which the event is appended. Currently, we use a straightforward LP $_{sender}$ modulo $_{tk}$ as the hash function. Consequently, enqueue involves just 1 extra modulo instruction over regular **ladderQ** and hence retains its amortized constant time complexity. Similar to buckets, the sub-buckets are implemented using standard **std::vector** with events added or removed only from the end to ensure amortized constant-time operation.

The dequeue operations for a bucket require iterating over each sub-bucket. However, for a small, fixed value of $_{tk}$, the overhead becomes an ammortized constant. The constant overhead is determined by the value of $_{tk}$. Consequently, dequeue also retains the amortized constant characteristic from regular **ladderQ** as summarized in Table 4. Currently, we do not subdivide *Bottom* but leave it as a possible future optimization.

4.7 Performance gain of 2tLadderQ

The primary performance gain for **2tLadderQ** arises from the reduced time complexity for event cancellation. Since each bucket is sub-divided, only $1 \div_{\mathrm{tk}}$ fraction of events need to be checked during cancellation. For example, if ${}_{\mathrm{t2}}k$=32, only $\frac{1}{32}$ of the pending events are scanned during cancellation. This significantly reduces the time constants in larger simulations enabling rapid rollback recovery.

The value of ${}_{\mathrm{t2}}k$ is a key parameter that influences the overall constants in **2tLadderQ**. For sequential simulation, where event cancellations do not occur, we recommend ${}_{\mathrm{t2}}k$=1. With this setting the performance of **2tLadderQ** is very close to that of the regular **ladderQ**. However, in parallel simulation, the value of ${}_{\mathrm{t2}}k$ must be greater than 1 to realize benefits of its design. Figure 4.6 shows the effect of changing the size of ${}_{\mathrm{t2}}k$ in a parallel simulation with 16 MPI processes. The total rollbacks in the simulations were with 10% (except for ${}_{\mathrm{t2}}k$=512, which for this model experienced fewer rollbacks). Nevertheless, for ${}_{\mathrm{t2}}k$=1, the simulation has *much* higher runtime due to event cancellation overheads. The runtime dramatically decreases as ${}_{\mathrm{t2}}k$ is increased. The runtime remains comparable for a broad range of values, namely: $64 \leq {}_{\mathrm{t2}}k <$. However, for ${}_{\mathrm{t2}}k \geq$, we noticed slow increase in runtime due to overhead of larger sub-buckets. Consequently, we have used a value of ${}_{\mathrm{t2}}k$=128 for parallel simulation. We anticipate ${}_{\mathrm{t2}}k$ value to vary depending on the hardware configuration of the compute cluster used for parallel simulation.

5 Related Work

Our research proposes and explores multi-tier data structures for managing the pending event set in sequential and optimistic parallel simulations. Specifically, we compare effectiveness of the data structures against our fine-tuned version of the Ladder Queue [11] because it has shown to be very efficient for sequential DES. Recently, Franceschini et al [8] compared several priority-queue based pending event data structures to evaluate their performance in the context of sequential DEVS simulations. They found that Ladder Queue outperformed every other priority queue based pending event data structure such as Sorted List, Minimal List, Binary Heap, Splay Tree, and Calendar Queue. Tang et al [11] and Franceschini et al [8] both use the classic Hold benchmark simulation model used in this study and described in Section 3.1.

In contrast to earlier work, rather than using a linked list based implementation, we propose alternative implementation using dynamically growing arrays (i.e. std::vector). Furthermore, we trigger *Bottom* to *Ladder* re-bucketing only if the *Bottom* has events at different timestamps to reduce inefficiencies. Our 2-tier Ladder Queue (**2tLadderQ**) is a novel enhancement to the Ladder Queue to enable its efficient use in optimistic parallel simulations.

Dickman et al [12] compare event list data structures that consisted of Splay Tree, STL Multiset and Ladder Queue. However, the focus of their paper was in developing a framework for handling pending event set data structure in shared memory PDES. A central component of their study was the identification of an appropriate data structure and design for the shared pending event set. Gupta et al [13] extended their implementation of Ladder Queue for shared memory Time Warp based simulation environment, so that it supports lock-free access to events in the shared pending event set. The modification involved the use of an unsorted lock-free queue in the underlying Ladder Queue structure. Marotta et al [14] have contributed to the study of pending event set data structures in threaded PDES through the design of the Non-Blocking Priority Queue (NBPQ) data structure. A pending event set data structure that is closely related to Calendar Queues with constant time performance.

In contrast to aforementioned efforts, our research focuses on distributed memory platforms in which each parallel process is single threaded. Consequently, our implementation does not involve thread synchronization issues. However, our 2-tier design has the ability to further reduce lock contention issues in multithreaded environments and could provide further performance boost. To the best of our knowledge, the Fibonnacci heap (**fibHeap**) and our 3-tier Heap (**3tHeap**) are unique data structures that have potential to be effective in simulations with high concurrency.

6 Experiments & Discussions

Assessments of the effectiveness of the six scheduler queues from Section 4 have been conducted using different configurations of the **PHOLD** benchmark discussed in Section 3.1. The experiments were conducted on the distributed memory compute cluster described in Section 2.1. Our initial experimental analysis proved to be time consuming due to the large number of **PHOLD** parameters (see Table 3.1) and combinations of their values. Consequently, we pursued strategies to focus on the most influential **PHOLD** parameters that impacted relative performance of the scheduler queues using Generalized Sensitivity Analysis (GSA) [15]. Section 6.1 discusses GSA experiments used to reduce the **PHOLD** parameter space and subsequent **PHOLD** configurations, called **ph3**, **ph4**, and **ph5**, used for further experiments. Section 6.2 discuss the results from sequential simulations conducted using **ph3**, **ph4**, and **ph5**.

6.1 Parameter reduction via GSA

Generalized Sensitivity Analysis (GSA) is based on two-sample Kolmogorov-Smirnov Test (KS-Test) and yields a $d_{m,n}$ statistic that is sensitive to differences in both central tendency and differences in the distribution functions of parameters [15]. The $d_{m,n}$ statistic is the maximum separation between cumulative probability distribution observed in a two-sample KS-Test. The KS-Test is performed with data from Monte Carlo simulations involving combinations of parameter values from a specified range or probability distribution. The simulation result is then classified into number of "success" (m) or its converse "failure" (n) to compute cumulative probability distribution and $d_{m,n}$ statistic for each parameter. In this study we have defined "failure" to be parameter values for which the **2tLadderQ** runs slower when compared to another scheduler queue. For sequential and parallel simulations we use ${}_{\mathrm{t2}}k$=1 and ${}_{\mathrm{t2}}k$=128 respectively.

An important aspect of GSA is to ensure that the values for each parameter covers its full range of values. Consequently, we use Sobol random numbers to select a combination of **PHOLD** parameter values to be used for simulation. Sobol random numbers are quasi-random low-discrepancy sequences that provide uniform coverage of a multidimensional parameter space for **PHOLD** (see Figure 3.1). Our parameter ranges also ensure that the peak memory consumption do not cross NUMA threshold, which in our case is 4 GB of RAM. Exceeding the 4 GB NUMA threshold introduces a lot of variance in runtimes requiring many runs to reduce variance to acceptable limits.

The randomly (using Sobol sequences) selected parameter set is used to run the model using two different scheduler queues. Average simulation execution time from 3 different replications is recorded for each scheduler queue along with the parameter-set. The process is repeated for 2,500 different Sobol sequences. The 2,500 data set is then collectively analyzed to compute the $d_{m,n}$ statistics for the different parameters. The results from sequential and parallel GSA are discussed in the following subsections.

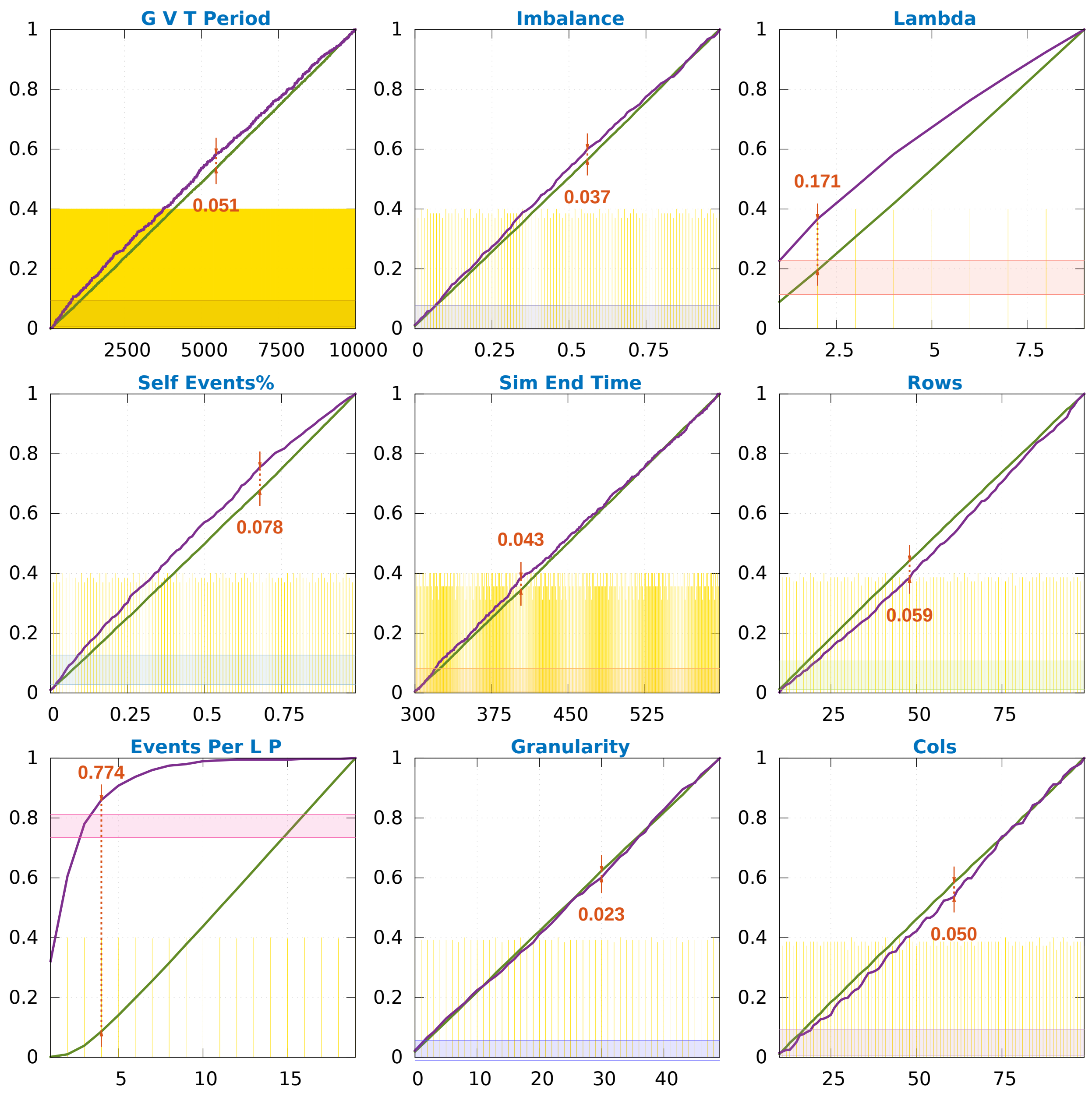

Figure 8: Results from Generalized Sensitivity Analysis (GSA) comparing 3tHeap and 2tLadderQ for sequential simulation.

6.1.1 GSA results for Sequential simulations

The charts in Figure 8 shows the cumulative m, n, and the $d_{m,n}$ statistics for the 9 different parameters explored using GSA for sequential simulations. The orange impulses show the parameter values and number of samples used for Monte Carlo simulation. Note that the distribution of samples varies depending on the nature of the parameter – *i.e.,* **eventsPerLP** varies in discrete steps of 1 from 1–20 while **imbalance** varies from 0 to 1.0 in small fractional steps.

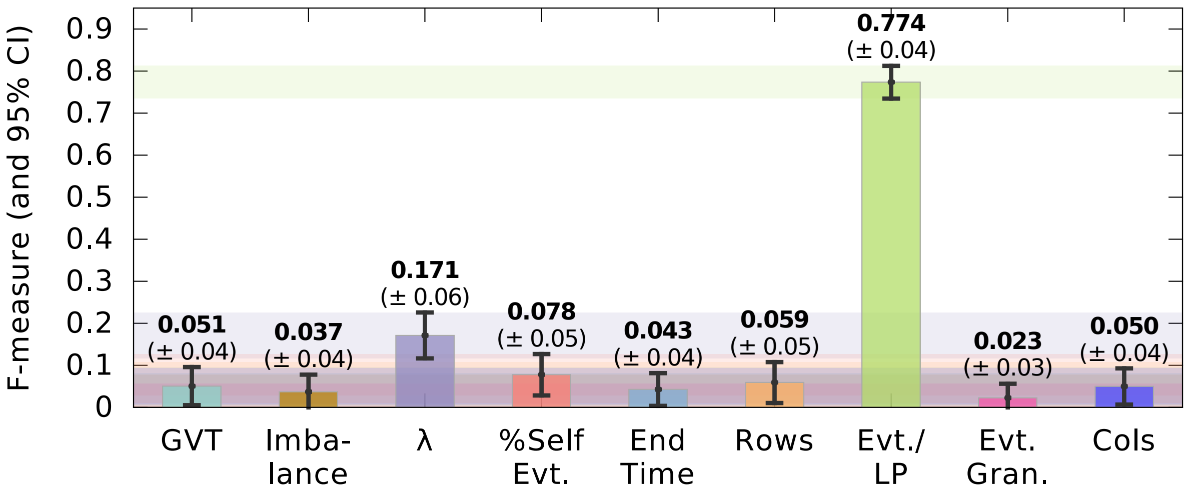

Figure 9: Summary of influential parameters from Figure 8 that cause performance differences between 2tLadderQ and 3tLadder in sequential simulations.

The chart in Figure 9 shows the summary of the $d_{m,n}$ statistic or influence of each parameter (see Table 3.1) on the outcome – *i.e.,* **2tLadderQ** performs better or worse than **3tHeap**. The lightly shaded bands show the 95% Confidence Intervals (CI) computed using standard bootstrap approach using 5000 replications with 1000 samples in each. As expected, the **imbalance** (*i.e.,* skew in partition) has no impact in sequential simulation and has a low impact score of 0.037. Similarly, the GVT computation rate does not impact pending events and consequently its influence is low at 0.051.

Interestingly, other model parameters such as **rows**, **cols**, **self-events**, **simEndTime**, and **granularity** have no influence on relative performance of **2tLadderQ** vs **3tHeap**. The parameter with most influence is **eventsPerLP** with a score of 0.774. This parameter determines total number of concurrent events which influences bucket sizes and number of rungs in **2tLadderQ** as well as the third tier size in **3tHeap**. The parameter λ for exponential distribution has a marginal influence because it influences number of concurrent events as discussed in Section 3.1 and shown in Figure 3.1(c).

We have also conducted GSA to determine influential parameters impacting performance of other scheduler queues versus the **2tLadderQ** in sequential simulations. Our analysis showed that none of the parameters play an influential role and the **2tLadderQ** performed consistently better or the same when compared to **ladderQ**, **2tHeap**, **fibHeap**, and **heap**. Only **3tHeap** and in few cases **2tHeap** outperformed our **2tLadderQ** in certain configurations. The performance of **ladderQ** and **2tLadderQ** was practically indistinguishable in sequential simulations (with $_{2\mathrm{t}}k$=1).

Summary: GSA shows that for comparing event queue performance in sequential simulations using our **PHOLD** benchmark, we just need to focus on 1 or 2 parameters. Other aspects such as: model size, event granularity, fraction of self-events, GVT rate, etc., do not matter for comparison of scheduler queues. The scheduler queues to focus further analysis are: **ladderQ**, **2tLadderQ**, and **3tHeap**.

6.1.2 GSA results for Parallel simulations

GSA for parallel simulations were conducted using the same procedure discussed earlier but using 4 MPI-processes for parallel simulation. These analysis focused only on **ladderQ**, **2tLadderQ**, and **3tHeap** based on the inferences drawn from the earlier analyses. The average simulation execution time from 3 replications is recorded for each scheduler queue along with the parameter set. Initially, we observed that the **ladderQ** timings showed a lot of variance in runtime depending on number of rollbacks that occur. Consequently, to reduce variance, we have used a time-window of 10 time-units to curtail optimism and reduce rollbacks. The time-window restricts the simulation kernel from scheduling events that are more than 10 time-units ahead of GVT. We use the same time-window for all scheduler queues for consistent comparison and analysis.

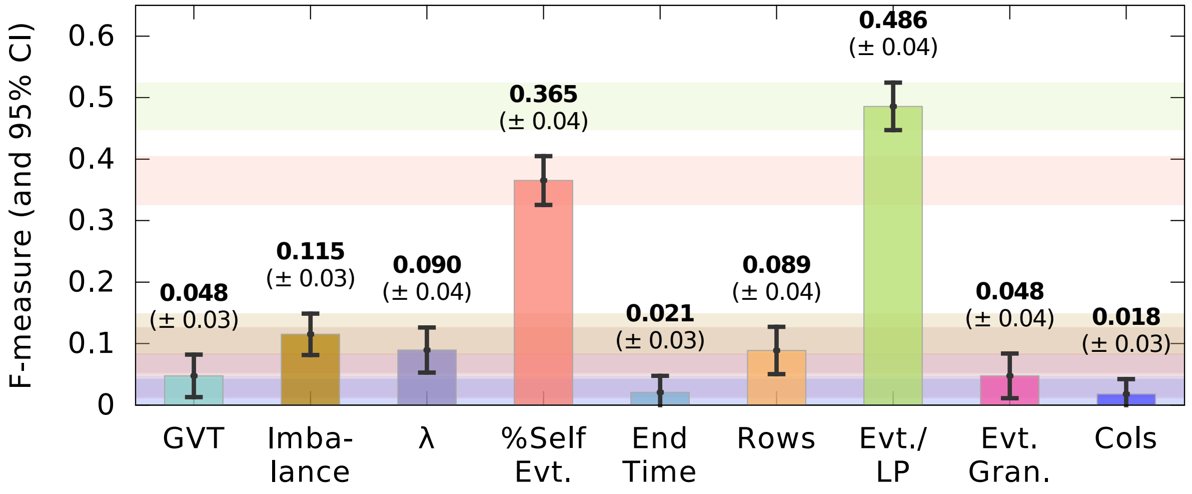

Figure 10: GSA data from parallel simulations (4 MPI-processes) showing influential parameters (2tLadderQ vs. 3tHeap).

The chart in Figure 10 shows the summary of the $d_{m,n}$ statistic or influence of each parameter (see Table 3.1) on the outcome – *i.e.,* **2tLadderQ** performs better or worse than **3tHeap**. The lightly shaded bands show the 95% Confidence Intervals (CI) computed using standard bootstrap approach using 5000 replications with 1000 samples in each. The parallel results are consistent with the sequential results and the **eventsPerLP** is the most influential parameter. However, in parallel simulation, the percentage of **selfEvents** (*i.e.,* LPs schedule events to themselves) has a more pronounced influence when compared to λ. The increased impact of **selfEvents** arises due to the use of optimistic synchronization. The self-events are local and can be optimistically processed, with some being rolled back, causing more operations on a larger pending event set. The data also shows that conspicuous **imbalance** in partitioning or load balance has some influence on the outcomes. However, in this study we explore typical parallel simulation scenarios in which load is reasonably well balanced.

6.1.3 PHOLD configurations for further analysis

The Generalized Sensitivity Analysis (GSA) enables identification of influential parameters, thereby substantially reducing the parameter space. However, GSA data does not provide an effective data set to analyze trends, such as: scalability, memory usage, rollback behaviors, etc. In order to pursue such analysis we

Table 3: Configurations used for further analysis

Name	#LPs (Rows×Cols)	Sim. End Time Seq	Sim. End Time Parallel
ph3	1,000 (100×10)	5000	20000
ph4	10,000 (100×100)	500	5000
ph5	100,000 (1000×100)	100	1000

have used 3 different **PHOLD** configurations called **ph3**, **ph4**, and **ph5**. The fixed characteristics for the 3 configurations with non-influential parameters is summarized in Table 3. We use larger simulation end times for parallel simulation so obtain sufficiently long runtimes using 32 cores. The value of influential parameters, namely: **eventsPerLP**, **%selfEvents**, and λ is varied for comparing different settings, similar to the approach used by other investigators [11, 8].

6.2 Sequential simulation results

Sequential simulations were conducted to assess the effectiveness of the different data structures. We pursued sequential simulations to compare the base case performance of the data structures, consistent with prior investigations [11, 8]. The sequential simulations also serve as a reference for potential use in conservatively synchronized PDES. The sequential experiments were conducted using 3 **PHOLD** configurations (see Section 6.1.3) on one compute node of our cluster described in Section 2.1. The simulations use only 1 MPI-process and states are not saved . Number of sub-buckets in **2tLadderQ** was set to 1, *i.e.,* ${}_{\mathrm{t2}}k$=1. For these experiments, the influential parameters **eventsPerLP**, λ, and **%selfEvents** were varied to explore their impact on relative performance of the data structures. Event **granularity** was set to zero resulting in a fine grained simulation. For each configuration, data from 10 independent replications were collected and analyzed.

The charts in Figure 6.2(a)–(c) show change in runtime characteristics as the most influential parameter **eventsPerLP** is varied, for λ=1 (widest range of timestamps) and **%selfEvents** = 0.25. This configuration was generally the best for **ladderQ**. As illustrated by Figure 6.2(a)–(c), the performance of **ladderQ** and **2tLadderQ** (${}_{\mathrm{2t}}k$=1) is comparable as expected. However, the **2tLadderQ** performs slightly (paired t-test p-value $<$ 0.05, *i.e.,* averages are not equal) better in some cases possibly due to improved caching resulting from smaller tier-2 sub-buckets. These two queues outperform the other queues for lower values of **eventsPerLP**.

However, the **3tHeap** generally outperforms the other queues (except for **2tHeap** in some cases) for

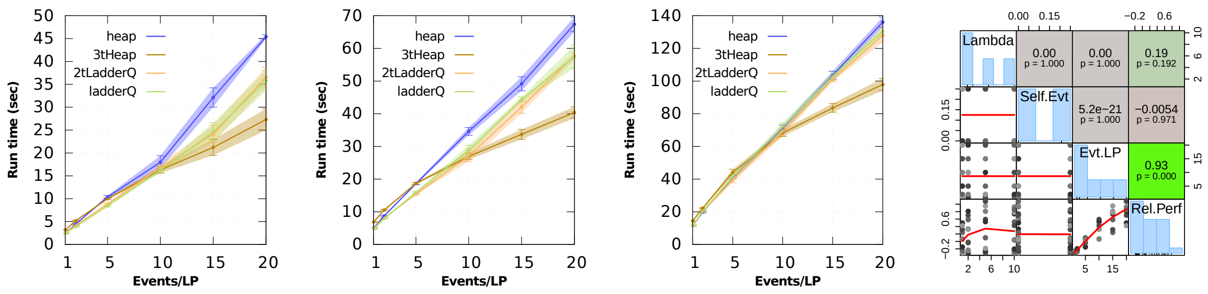

(a) **ph3** (b) **ph4** (c) **ph5** (d) Corellogram

Figure 11: Sequential simulation runtimes and correlation of 3tHeap performance with PHOLD parameters

higher values of **eventsPerLP**. In all cases, there were no inserts into *Bottom* or *Bottom*-to-*Ladder* operations (discussed in Section 4.5.1) that degrade **ladderQ** performance. The size of the *Bottom* rung was proportional to the number of LPs and **eventsPerLP** – *i.e.,* with larger models, *Bottom* has more events for many LPs with the same time stamp to be scheduled. In the larger configurations, the maximum of 8 rungs were fully used. The maximum rung threshold of 8 was determined to be an effective setting as discussed in Section 4.5.1 and the same value proposed by Tang et al [11].

Profiler data showed that the bottleneck in **ladderQ** arises from the overhead of re-bucketing events from rung-to-rung of the Ladder. On the other hand, in **3tHeap** re-bucketing does not occur. Consequently, the overheads of O(log $\frac{e}{c}$) operations in **3tHeap** are amortized as number of concurrent events c increases.

The chart in Figure 6.2(d) shows the correlation between the 3 influential parameters and the performance difference between **3tHeap** and **ladderQ**. Consistent with the GSA results, the correlogram shows that the most influential parameter is **eventsPerLP** (R=0.93, p=0) followed by λ (R=0.19, p=0.192) with a very weak correlation. The **%selfEvents** has practically no impact on performance. The correlogram also shows that these parameters are independent and have no covariance between each other (R $\sim$ 0, p >0.95).

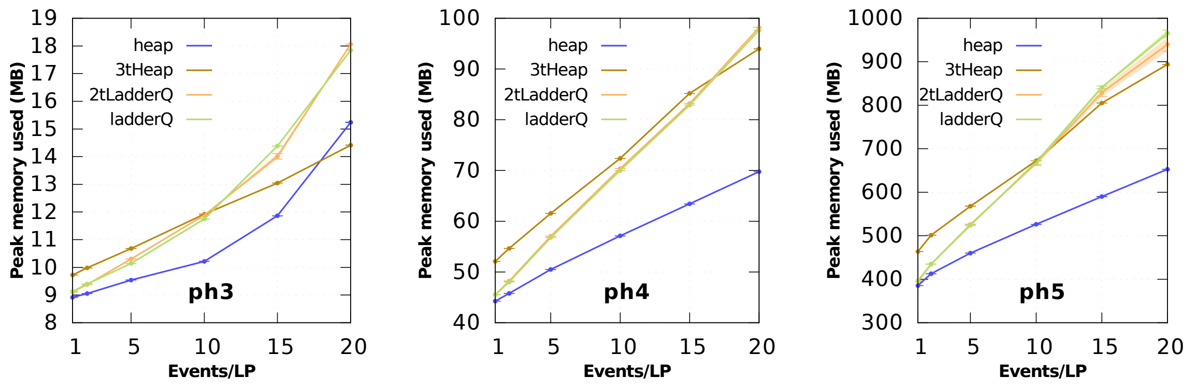

Figure 12: Comparison of peak memory usage

The charts in Figure 12 shows the peak memory usage corresponding to the runtime data in Figure 6.2. The memory size reported is the "Maximum resident set size" value reported by GNU **/usr/bin/time** command on Linux. The memory usage of **heap** is the lowest in most cases. Since ${}_{2\mathrm{t}}k{=}1$, the memory usage of **ladderQ** and **2tLadderQ** is comparable as expected. The **3tHeap** initially uses more memory than the other data structures because of many small **std::vector**s and due to **std::vector** doubling its capacity. However, the memory usage is amortized as the **eventsPerLP** increases. Consequently, the improved performance of **3tHeap** over **ladderQ** is realized without significant increase in memory footprint.

6.3 Parallel simulation assessments

The sequential simulation assessments indicated that **ladderQ**, **2tLadderQ**, and **3tHeap** performed the best for a broad range of **PHOLD** parameter settings. Consequently, we focused on assessing the effectiveness of these 3 queues for Time Warp synchronized parallel simulations. The experiments were conducted on our compute cluster (see Section 2.1) using a varying number of MPI-processes, with one process per CPU-core. In order to ensure sufficiently long runtimes with 32-cores, we increased **simEndTime** for parallel simulations as tabulated in Table 3. The following subsections discuss results from the experiments.

6.3.1 Throttling optimism with a time-window

Initially we conducted experiments with fine-grained setting (*i.e.,* **granularity** = 0) from sequential simulations. We noticed that the **ladderQ** had a large variance in runtimes, particularly when it experienced many rollbacks. In several cases, cascading rollbacks significantly slowed the simulations – *i.e.,* **ladderQ** simulations required over 1 hour while **2tLadderQ** would consistently finish in a few minutes. In order

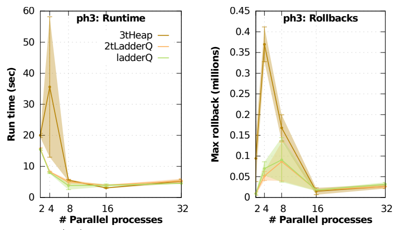

(a) **ph3** time & rollbacks

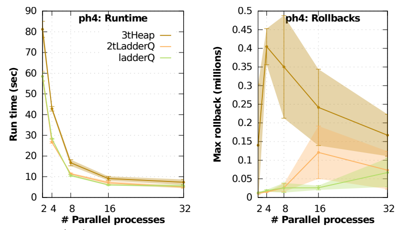

(b) **ph4** time & rollbacks

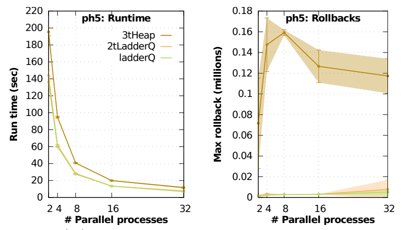

(c) **ph5** time & rollbacks

Figure 13: Statistics from parallel simulation with eventsPerLP=2, $\lambda = 1$, %selfEvents=25%

to avoid such debilitating rollback scenarios and to streamline experimental analysis timeframes we have throttled optimism using a time-window of 10 time-units. The time-window restricts the simulation kernel from scheduling events that are more than 10 time-units ahead of GVT. The time-window value of 10 is 50% of the maximum timestamp of events generated by exponential distribution with $\lambda = 1$. Consequently, most events in current schedule cycle will fit within this time-window with limited impact on concurrency. We use the same time-window for all scheduler queues for consistent comparison and analysis.

6.3.2 Efficient case for ladderQ

The charts in Figure 13 show key simulation statistics for low value of **eventsPerLP** $= 2$ and λ=1 for which **ladderQ** performed well, consistent with the observations in sequential simulations. The statistics show average and 95% CI computed from 10 independent replications for each data point. The peak rollbacks among all of the MPI-processes is shown as it controls overall progress in the parallel simulations. As illustrated by the data in Figure 13, both the **ladderQ** and **2tLadderQ** perform well for all three models. In this configuration, overall the **ladderQ** experienced the fewest rollbacks. Nevertheless, the **2tLadderQ** continues to perform well despite experiencing more rollbacks as shown in Figure 13(b). The good performance of **2tLadderQ** under heavy rollback is consistent with its design objective to enable rapid event cancellation and improve rollback recovery. The maximum of 8 rungs on the ladder was reached in all the simulations, but with only few (1 to 3) buckets per rung. On average, the number of *Bottom* to Ladder operations (that degrade performance) were low per MPI process, about – **ph3**: {9144, 8911}, **ph4**: {1904, 1448}, and **ph5**: {53, 84} for {**ladderQ**, **2tLadderQ**} respectively. We did not observe a strong correlation between number of these operations and rollbacks.

In this configuration, the **3tHeap** runs experienced a lot of rollbacks when compared to the other two queues despite the time-window. For **ph5** data in Figure 13(c), **3tHeap** experienced about 114805 rollbacks on average while **ladderQ** experienced only 2341, almost 50×fewer rollbacks. Consequently, it was slower

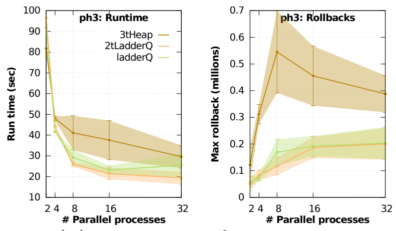

(a) **ph3** time & rollbacks

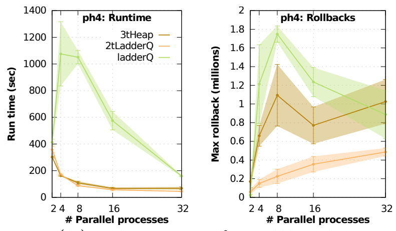

(b) **ph4** time & rollbacks

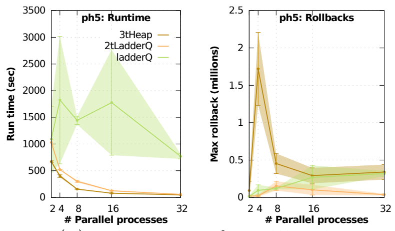

(c) **ph5** time & rollbacks

Figure 14: Statistics from parallel simulation with eventsPerLP=10, $\lambda = 10$, %selfEvents=25%

than the other 2 queues, but its performance is not significantly degraded – $\tilde{1}.5\times$ slower despite $50\times$ more rollbacks. The peak memory usage for all the 3 queues was comparable in these configurations.

6.3.3 Knee point for 3tHeap vs. ladderQ

The charts in Figure 14 show key simulation statistics for the configuration where **3tHeap** and **ladderQ** performed about the same in sequential (see Figure 6.2). For **ph3**, both **ladderQ** and **2tLadderQ** experienced comparable number of rollbacks but the **2tLadderQ** performs better due to its design advantages. In the case of **ph4** and **ph5**, both the **ladderQ** and **3tHeap** experienced a comparable number of rollbacks, but much higher than the **2tLadderQ** despite having a time-window. Nevertheless, the **3tHeap** conspicuously outperforms the **ladderQ** because it is able to quickly cancel events and complete rollback processing. For **ph5**, the **3tHeap** outperforms the other 2 queues despite the high number of rollbacks. The peak memory usage for all the 3 queues was comparable in these configurations.

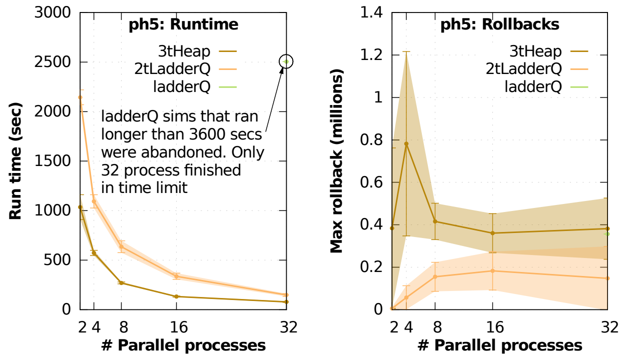

Figure 15: ph5 Statistics (best case for 3tHeap)

6.3.4 Best case for 3tHeap

Figure 15 shows simulation time and rollback characteristics in high concurrency configuration with **ph5**, with **eventsPerAgent**=20, λ=10, and **%Self Evt.**=25%. The **ladderQ** runs exceeded 3600 seconds in most cases even with a time-window, except for 32 processes. Consequently **ladderQ** experiments with fewer than 32 processes were abandoned. On the other hand **2tLadderQ** performed well due to its design. The **3tHeap** outperformed the other 2 queues despite experiencing $2\times$ more rollbacks.

7 Plan of Action and Milestones

This section describes the work that needs to be conducted to complete the research thesis.

❶ **Implement 2 additional simulation models**: The experimental analysis was conducted using PHOLD. We will extend the experimental analysis to include 2 additional models in order to evaluate performance of the data structures across different simulation models. The 2 simulation models will be implemented by 30 March 2017.

❷ **Assessment using additional simulation models**: The assessment of data structure performance using the models in sequential and optimistic parallel simulations will be completed by 28 April 2017.

❸ **Record experimental results and analysis**: The research thesis writing will be completed by 19 May 2017 in preparation for the thesis defense.

References

[1] G. Fishman, *Discrete-event simulation: modeling, programming, and analysis.* Springer Science & Business Media, 2013.

[2] R. M. Fujimoto, "Parallel discrete event simulation," *Communications of the ACM*, vol. 33, no. 10, pp. 30–53, 1990.

[3] R. R. Hill, J. O. Miller, and G. A. McIntyre, "Simulation analysis: applications of discrete event simulation modeling to military problems," in *Proceedings of the 33nd conference on Winter simulation*, pp. 780–788, IEEE Computer Society, 2001.

[4] S. Jafer, Q. Liu, and G. Wainer, "Synchronization methods in parallel and distributed discrete-event simulation," *Simulation Modelling Practice and Theory*, vol. 30, pp. 54–73, 2013.

[5] D. W. Jones, "An empirical comparison of priority-queue and event-set implementations," *Communications of the ACM*, vol. 29, no. 4, pp. 300–311, 1986.

[6] R. Rönngren and R. Ayani, "A comparative study of parallel and sequential priority queue algorithms," *ACM Transactions on Modeling and Computer Simulation (TOMACS)*, vol. 7, no. 2, pp. 157–209, 1997.

[7] R. Brown, "Calendar queues: a fast 0 (1) priority queue implementation for the simulation event set problem," *Communications of the ACM*, vol. 31, no. 10, pp. 1220–1227, 1988.

[8] R. Franceschini, P.-A. Bisgambiglia, and P. Bisgambiglia, "A comparative study of pending event set implementations for pdevs simulation," in *Proceedings of the Symposium on Theory of Modeling & Simulation: DEVS Integrative M&S Symposium*, DEVS '15, (San Diego, CA, USA), pp. 77–84, Society for Computer Simulation International, 2015.

[9] C. D. Carothers and K. S. Perumalla, "On deciding between conservative and optimistic approaches on massively parallel platforms," in *Proceedings of the Winter Simulation Conference*, WSC '10, pp. 678–687, Winter Simulation Conference, 2010.

[10] J.-S. Yeom, A. Bhatele, K. Bisset, E. Bohm, A. Gupta, L. V. Kale, M. Marathe, D. S. Nikolopoulos, M. Schulz, and L. Wesolowski, "Overcoming the scalability challenges of epidemic simulations on blue waters," in *Parallel and Distributed Processing Symposium, 2014 IEEE 28th International*, pp. 755–764, IEEE, 2014.

[11] W. T. Tang, R. S. M. Goh, and I. L.-J. Thng, "Ladder queue: An o(1) priority queue structure for large-scale discrete event simulation," *ACM Trans. Model. Comput. Simul.*, vol. 15, pp. 175–204, July 2005.

[12] T. Dickman, S. Gupta, and P. A. Wilsey, "Event pool structures for pdes on many-core beowulf clusters," in *Proceedings of the 1st ACM SIGSIM Conference on Principles of Advanced Discrete Simulation*, SIGSIM PADS '13, (New York, NY, USA), pp. 103–114, ACM, 2013.

[13] S. Gupta and P. A. Wilsey, "Lock-free pending event set management in time warp," in *Proceedings of the 2Nd ACM SIGSIM Conference on Principles of Advanced Discrete Simulation*, SIGSIM PADS '14, (New York, NY, USA), pp. 15–26, ACM, 2014.

[14] R. Marotta, M. Ianni, A. Pellegrini, and F. Quaglia, "A non-blocking priority queue for the pending event set," in *Proceedings of the 9th EAI International Conference on Simulation Tools and Techniques*, SIMUTOOLS'16, (ICST, Brussels, Belgium, Belgium), pp. 46–55, ICST (Institute for Computer Sciences, Social-Informatics and Telecommunications Engineering), 2016.

[15] B. Guven and A. Howard, "Identifying the critical parameters of a cyanobacterial growth and movement model by using generalised sensitivity analysis," *Ecological Modelling*, vol. 207, no. 1, pp. 11 – 21, 2007.